Multi-Objective Road Adaptive Control of an Active Suspension System

Guido Koch, Klaus J. Diepold and Boris Lohmann

Abstract In the design of automobile suspension systems, the classical conflict between minimizing vertical chassis acceleration to increase passenger comfort and keeping the dynamic wheel load small in order to ensure safe driveability must be further eased due to increasing customer demands. In order to moderate the conflicting suspension objectives, a switching controller structure for an active suspension system is developed which schedules linear optimal regulators depending on the present dynamic wheel load and suspension deflection. The goal is to maximize ride comfort while the wheel load is below certain safety critical bounds and the suspension deflection remains within given construction-conditioned limits. Stability of the switching control system is analyzed using a multiple Lyapunov function approach. The performance of the road adaptive suspension control system is compared with a linear controller and the passive suspension system in simulations to point out the benefits of the developed control concept.

1 Introduction

An automotive suspension system is expected to provide an optimum of ride comfort for the passengers as well as safe driveability of the car, i.e. guaranteed tire-road contact. While the comfort aspect can be characterized by minimum vertical chassis acceleration, the safety aspect requires a stiff, well damped coupling between vehicle and road in order to keep dynamic wheel load deviations small. Another objective is that the suspension deflection should always remain below the constructionally given limits in order to prevent impulse-like accelerations of the suspended mass as well as excessive wear of the components. These three requirements are con-

Guido Koch, Klaus J. Diepold and Boris Lohmann
Institute of Automatic Control, Technische Universität München, 85748 Garching bei München, Germany; E-mail: guido.koch@tum.de, kj.diepold@mytum.de, lohmann@tum.de

H. Ulbrich and L. Ginzinger (eds.), Motion and Vibration Control, 189–200.

flicting, [2]. However, this conflict can be eased by controlled actuators in active suspension systems.

Some works on suspension controller design present the idea of adapting the control objectives and thus the controller dynamics to the current road excitation. In [1,4,5] switching controllers are presented that minimize either the vertical chassis acceleration or the suspension deflection. In [9], a control structure with adaptive properties has been presented using a wheel load adaptive skyhook-control concept for a *semi-active* suspension system.

The new approach in this paper is the design of a nonlinear controller structure that adapts to the current road disturbance in order to optimize the suspension regarding the three conflicting objectives comfort, safe driveability and suspension deflection limits. The main idea is that maximum comfort should be achieved while safety for every road excitation is preserved by keeping the dynamic wheel load and the suspension deflection below specified critical bounds. This is accomplished by a switching controller structure based on six linear quadratic optimal controllers and a switching logic. The required actuator force for control should be feasible.

The remainder of this paper is organized as follows: First, models for an active and passive vehicle suspension are presented in Section 2 and performance requirements are specified. In Section 3, the controller structure and the calculation of the scheduling variables initializing the switching are presented. Stability of the switched control system for the active suspension is analyzed in Section 4 using a multiple Lyapunov function approach. Finally, simulation results and a performance comparison are presented.

2 Modelling and System Requirements

The lift movement of the suspension system can be modelled using the well-known quarter car models illustrated in Figure 1 [7, 11]. In the high bandwidth active suspension considered here an ideal actuator is integrated.

The model of the passive suspension results from the active suspension model if $F(t) = 0$. The state-vector $\mathbf{x}$ and the output vector $\mathbf{y}$ are introduced as $\mathbf{x} =$

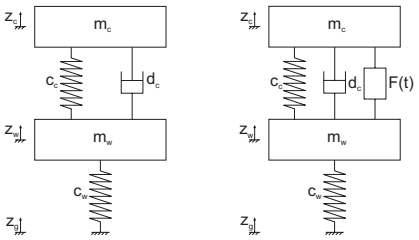

Fig. 1 Quarter car models of the passive (left) and active suspension (right).

Table 1 Notation and parameter values [7].

Model parameter	Symbol	Value	Unit
Quarter car chassis mass (sprung mass)	m_c	256	[kg]
Wheel assembly mass (unsprung mass)	m_w	31	[kg]
Suspension spring stiffness	c_c	20200	[N/m]
Tire stiffness	c_w	128000	[N/m]
Sprung mass damping coefficient	d_c	1140	[Ns/m]
Undamped uncoupled natural frequency of the sprung mass	$\omega_c = \sqrt{\frac{c_c}{m_c}}$	8.88	[rad/s]
Uncoupled natural frequency of the unsprung mass	$\omega_w = \sqrt{\frac{c_w}{m_w}}$	64.26	[rad/s]

$[\, z_c - z_w,\ \dot{z}_c,\ z_w - z_g,\ \dot{z}_w \,]^T$ and $\mathbf{y} = [\, \ddot{z}_c,\ F_{dyn},\ z_c - z_w \,]^T$ where F_{dyn} denotes the dynamic wheel load force. With the control input $u(t) = F(t)$ and disturbance input $u_d(t) = \dot{z}_g(t)$ the quarter-car model can be expressed as a state space model in the form

$$\dot{\mathbf{x}} = \mathbf{A}\mathbf{x} + \mathbf{b}u + \mathbf{e}u_d \ , \qquad \mathbf{y} = \mathbf{C}\mathbf{x} + \mathbf{d}u \ , \tag{1}$$

$$\mathbf{A} = \begin{bmatrix} 0 & 1 & 0 & -1 \\ -\frac{c_c}{m_c} & -\frac{d_c}{m_c} & 0 & \frac{d_c}{m_c} \\ 0 & 0 & 0 & 1 \\ \frac{c_c}{m_w} & \frac{d_c}{m_w} & -\frac{c_w}{m_w} & -\frac{d_c}{m_w} \end{bmatrix}, \ \mathbf{b} = \begin{bmatrix} 0 \\ \frac{1}{m_c} \\ 0 \\ -\frac{1}{m_w} \end{bmatrix}, \ \mathbf{e} = \begin{bmatrix} 0 \\ 0 \\ -1 \\ 0 \end{bmatrix}, \tag{2}$$

$$\mathbf{C} = \begin{bmatrix} -\frac{c_c}{m_c} & -\frac{d_c}{m_c} & 0 & \frac{d_c}{m_c} \\ 0 & 0 & c_w & 0 \\ 1 & 0 & 0 & 0 \end{bmatrix}, \ \mathbf{d} = \begin{bmatrix} \frac{1}{m_c} \\ 0 \\ 0 \end{bmatrix} . \tag{3}$$

The model parameters are given in Table 1.

2.1 Performance Requirements

In order to ensure maximum ride comfort, the rms-value of the vertical chassis acceleration $\|\ddot{z}_c\|_{rms}$ is to be minimized. The human sensitivity for vibration is frequency dependent and the most sensitive frequency range for mechanical excitation is 4–8 Hz [3]. Therefore, a fifth order shaping filter $G_c(j\omega)$ with an amplitude characteristic as depicted in Figure 2 and a state space representation

$$\dot{\mathbf{x}}_f = \mathbf{A}_f\mathbf{x}_f + \mathbf{b}_f\ddot{z}_c \ , \quad \ddot{z}_{c,f} = \mathbf{c}_f^T\mathbf{x}_f \tag{4}$$

is introduced, [3]. Its impulse response is $g_c(t)$ such that $\ddot{z}_{c,f} = g_c(t) * \ddot{z}_c$.

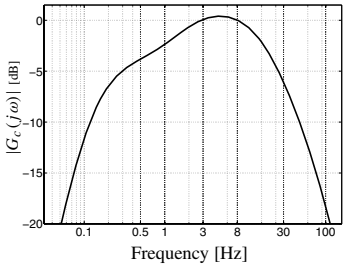

Fig. 2 Amplitude characteristic of the shaping filter $G_c(j\omega)$ [3].

An augmented plant model with state vector $\mathbf{x}_{reg} = [\,\mathbf{x}^T,\ \mathbf{x}_f^T\,]^T$ is used to incorporate the shaping filter in the controller design (Section 3) such that the controlled variables are $\mathbf{y}_{reg} = [\,\ddot{z}_{c,f},\ \ddot{z}_c,\ F_{dyn},\ z_c - z_w\,]^T$. With $\mathbf{h} = [\,0\ 1\ 0\ 0\,]$ the augmented plant model is

$$\dot{\mathbf{x}}_{reg} = \underbrace{\begin{bmatrix} \mathbf{A} & \mathbf{0} \\ \mathbf{b}_f\mathbf{h}\mathbf{A} & \mathbf{A}_f \end{bmatrix}}_{\mathbf{A}_{reg}} \mathbf{x}_{reg} + \underbrace{\begin{bmatrix} \mathbf{b} \\ \mathbf{b}_f\mathbf{h}\mathbf{b} \end{bmatrix}}_{\mathbf{b}_{reg}} u + \underbrace{\begin{bmatrix} \mathbf{e} \\ \mathbf{0} \end{bmatrix}}_{\mathbf{e}_{reg}} u_d \quad , \tag{5}$$

$$\mathbf{y}_{reg} = \underbrace{\begin{bmatrix} \mathbf{0} & \mathbf{c}_f^T \\ \mathbf{C} & \mathbf{0} \end{bmatrix}}_{\mathbf{C}_{reg}} \mathbf{x}_{reg} + \underbrace{\begin{bmatrix} \mathbf{0} \\ \mathbf{d} \end{bmatrix}}_{\mathbf{d}_{reg}} u \ . \tag{6}$$

Safety requirements

For stochastic road excitation the dynamic wheel load's rms-value should be bounded as follows[1]

$$\max\left(\|F_{dyn}\|_{rms}\right) \le \Gamma_{var} = \frac{F_{stat}}{3} \ , \tag{7}$$

where $F_{stat} = g\,(m_c + m_w)$ denotes the static wheel load. To ensure safety for singular excitation events like potholes, the primary control objective changes from comfort to safety, i.e. dynamic wheel load limitation, if

$$\frac{|F_{dyn}|}{F_{stat}} \ge \Gamma_{sing} = 0.75 \ . \tag{8}$$

[1] This is derived from the 3σ-rule and assures, assuming a normally distributed stochastic disturbance signal, that F_{dyn} remains within $\pm F_{stat}$ for 99.7% of the time [10].

Requirements on suspension deflection

A total of $|\Delta\hat{z}| = 0.1\,\text{m}$ maximum suspension deflection is used as a limit in the simulations of this study. Hitting the limit is modelled by an increase in c_c as follows

$$\tilde{c}_c = \begin{cases} c_c & \text{for} \quad -0.1 \le z_c - z_w \le 0.1 \\ 15 \cdot c_c & \text{for} \quad |z_c - z_w| > 0.1 \wedge \ \dot{z}_c - \dot{z}_w > 0\,. \end{cases} \tag{9}$$

3 Controller Design

For the road adaptive suspension control $n = 6$ linear quadratic optimal (LQR) controllers with different weighting matrices $\mathbf{Q}_y$ for separate primary control objectives are designed in order to analyze the potential of the concept. For the application of the classical LQR design formalism with output weighting in the cost functional

$$J_{LQR} = \int_0^\infty \left(\mathbf{y}_{reg}^T \mathbf{Q}_y \mathbf{y}_{reg} + u R u\right) dt \tag{10}$$

with $\mathbf{Q}_y = \mathbf{Q}_y^T \ge 0$ and $R > 0$ chosen according to Table 2, the cost functional needs to be slightly modified due to the direct feedthrough term $\mathbf{d}_{reg}$ present in the augmented suspension model. The resulting cost functional resulting from Eq. (10) is

$$J_{LQR} = \int_0^\infty \left(\mathbf{x}_{reg}^T \mathbf{Q} \mathbf{x}_{reg} + 2\mathbf{x}_{reg}^T \mathbf{s} u + u \tilde{R} u\right) dt \tag{11}$$

with $\mathbf{Q} = \mathbf{C}_{reg}^T \mathbf{Q}_y \mathbf{C}_{reg}$, $\mathbf{s} = \mathbf{C}_{reg}^T \mathbf{Q}_y \mathbf{d}_{reg}$ and $\tilde{R} = \mathbf{d}_{reg}^T \mathbf{Q}_y \mathbf{d}_{reg} + R$. We substitute the control input $\tilde{u} = u + \tilde{R}^{-1} \mathbf{s}^T \mathbf{x}$ in Eq. (11) in order to remove the mixed term $2\mathbf{x}_{reg}^T \mathbf{s} u$ such that the conventional LQR design formalism can be applied [6]. The optimal solution for each designed LQR-controller with weighting matrix $\mathbf{Q}_{y,i}$ is state feedback $u_i = -\mathbf{k}_i^T \mathbf{x}_{reg}$ with $\mathbf{k}_i^T = \tilde{R}^{-1}(\mathbf{b}_{reg}^T \mathbf{P}_{r,i} + \mathbf{s}_i^T)$ and $\mathbf{P}_{r,i}$ being the symmetric, positive definite solution of the algebraic Riccati-equation

$$\begin{aligned} &\mathbf{A}^T \mathbf{P}_{r,i} + \mathbf{P}_{r,i} \mathbf{A} - \left(\mathbf{P}_{r,i} \mathbf{b}_{reg} + \mathbf{s}_i\right) \tilde{R}^{-1} \left(\mathbf{b}_{reg}^T \mathbf{P}_{r,i} + \mathbf{s}_i^T\right) + \mathbf{Q}_i = \mathbf{0}\,, \\ &\mathbf{P}_{r,i} = \mathbf{P}_{r,i}^T > \mathbf{0}\,. \end{aligned} \tag{12}$$

Wheel load adaptation

Figure 3 shows the control structure in which the LQR-controllers are implemented. In the following the part of the switching logic is presented that schedules the controllers by the scheduling variable $q_{adp}(t)$ with $0 \le q_{adp}(t) \le 1$ depending on the dynamic wheel load. The basic concept is described in [9] but is modified here

Table 2 Controller weights $\mathbf{Q}_{y,i}$, $R = 1$ for all controllers.

$\mathbf{Q}_{y,i}$	Value	Controller Type
$\mathbf{Q}_{y,1}$	$diag\left(3.5 \cdot 10^5, 0,\ 0.1,\ 0\right)$	Most comfort oriented controller
$\mathbf{Q}_{y,2}$	$diag\left(8 \cdot 10^4,\ 0,\ 0.4,\ 0\right)$	Comfort oriented controller
$\mathbf{Q}_{y,3}$	$diag\left(4 \cdot 10^4,\ 0,\ 0.7,\ 0\right)$	Intermediate controller
$\mathbf{Q}_{y,4}$	$diag\left(10^4,\ 0,\ 0.9,\ 0\right)$	Safety oriented controller
$\mathbf{Q}_{y,5}$	$diag(10,\ 0,\ 1,\ 0)$	Most safety oriented controller
$\mathbf{Q}_{y,6}$	$diag\left(0,\ 5.2 \cdot 10^7,\ 10^{-3},\ 3 \cdot 10^{12}\right)$	Suspension deflection controller

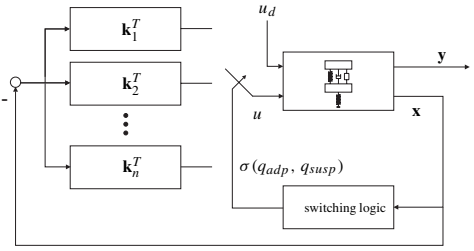

Fig. 3 Switching state feedback controller structure.

in details. In case of "hard" switching between the five comfort/safety oriented controllers $\mathbf{k}_i^T$, $i \in \{1, \ldots, 5\}$ (see Table 2) the piecewise continuous switching function is

$$\sigma\left(q_{adp}\left(t\right)\right) = \begin{cases} \lceil q_{adp}(t) \cdot 5 \rceil & \text{if} \quad 0 < q_{adp} \leq 1 \\ 1 & \text{if} \quad q_{adp} = 0 \end{cases} \tag{13}$$

where $\lceil \cdot \rceil$ denote Gaussian brackets also known as the ceiling function. The sixth controller is activated separately as described at the end of this section. The scheduling variable $q_{adp}(t)$ increases with increasing wheel load and correspondingly as $q_{adp}(t) \approx 1$, the most safety oriented controller $\mathbf{k}_5^T$ is chosen by the switching logic.

The current value of the scheduling variable is determined by two adaptation-rates as $q_{adp}(t) = \min(1, q_s(t) + q_f(t))$. The slow adaptation rate $q_s(t)$ (illustrated in the lower branch of block diagram in Figure 4) is used to adapt the suspension controller to different variances of the road excitation signal. The variance of the dynamic wheel load is

$$\sigma_{F_{dyn}}^2 = \lim_{T \to \infty} \frac{1}{T} \int_0^T F_{dyn}^2 dt.$$

After Laplace transformation we replace the integral term $\frac{1}{s}$ by a first order low pass filter thus approximating the dynamic wheel load's variance by

$$\sigma_{F_{dyn}}^2(s) \approx \frac{1}{\tau_s s + 1} F_{dyn}^2(s).$$

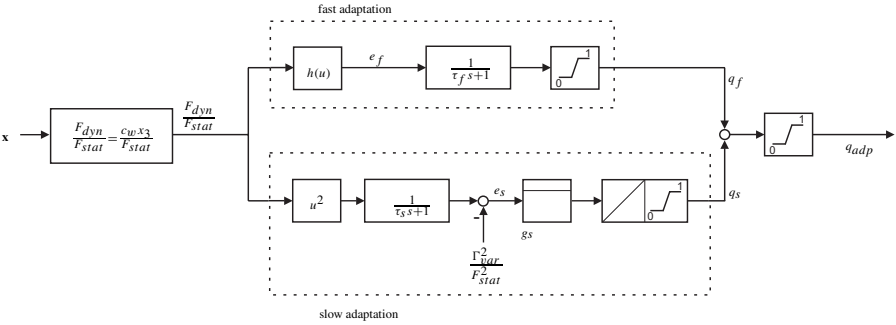

Fig. 4 Wheel load adaptation structure.

For τ_s the chassis mass eigenmodes' time constant is chosen resulting in $\tau_s = 2\pi\sqrt{m_c/c_c} \approx 0.71$ sec.

The dynamic wheel load filtered in this manner is compared to the upper bound Γ_{var} given by Eq. (7). The deviation

$$e_s(t) = \frac{\sigma^2_{F_{dyn}(t)}}{F^2_{stat}} - \frac{\Gamma^2_{var}}{F^2_{stat}}$$

is scaled by a constant $g_s = 1.5$ and is integrated by an output-limited integrator with an output signal range of [0, 1] resulting in q_s.

If the vehicle hits an occasional pothole on an otherwise smooth road, it is important that an instant switching to a safety oriented controller occurs. Therefore, it is necessary to introduce a fast adapting term $q_f(t)$ in the calculation of $q_{adp}(t)$ which is shown in the upper branch of the block diagram (Figure 4).

To ensure that this fast adaptation part remains inactive as long as the relative dynamic wheel load has not reached $\Gamma_{sing} = 0.75$ defined in Eq. (8), the wheel load is scaled by a nonlinear funtion h (based on a fourth order polynomial) shown in Figure 5 which output value e_f is only nonzero if $|F_{dyn}|/F_{stat} > 0.75$. Again a low pass filter for e_f with a time constant

$$\tau_f = \frac{5}{9} \cdot 2\pi \sqrt{\frac{m_w}{c_c + c_w}} \approx 0.05 \text{ sec}$$

is used. The output q_f is limited to a range of $q_f \in [0, 1]$ as well.

Suspension deflection adaptation

A second scheduling variable $q_{susp}(t)$ is calculated which determines when the sixth controller that suppresses excessive suspension deflection is activated by

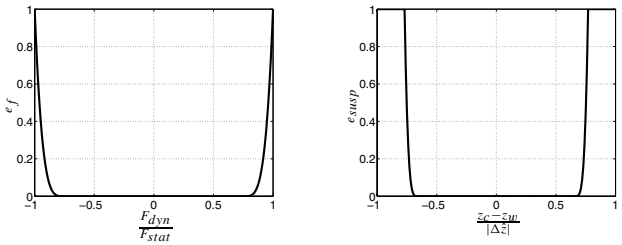

Fig. 5 Nonlinear scaling function $h(F_{dyn}/F_{stat})$ for fast wheel load adaptation (left) and $f(z_c - z_w/|\Delta\hat{z}|)$ for suspension deflection adaptation (right).

$\sigma(q_{adp}, q_{susp})$. This is described in detail in Section 4 because its switching behaviour determines the stability of the system. The scheduling variable $q_{susp}(t)$ is calculated similarly to $q_f(t)$ with $z_c - z_w/|\Delta\hat{z}|$ as input. Again a nonlinear function $f(z_c - z_w/|\Delta\hat{z}|)$ shown in Figure 5 is used being nonzero if $|z_c - z_w|/|\Delta\hat{z}| > 0.66$. The filter's time constant is $\tau_{susp} = 1/25\,\tau_f$ to ensure quick activation of the suspension deflection controller.

4 Stability Analysis

Stability analysis of switched systems is a very important issue because it is not guaranteed that switching between asymptotically stable subsystems (here: resulting from different controllers) results in an asymptotically stable switched system. A well known stability analysis approach uses quadratic Lyapunov functions of the form $V(\mathbf{x}) = \mathbf{x}^T\mathbf{P}\mathbf{x}$, $V(\mathbf{0}) = 0$, $V(\mathbf{x}) > 0$, $\dot{V}(\mathbf{x}) < 0$, $\mathbf{P} = \mathbf{P}^T > \mathbf{0}$. If a matrix $\mathbf{P}$ can be found such that these equations are fullfilled, the equilibrium $\mathbf{x} = \mathbf{0}$ of the switched system is uniformly asymptotically stable, [8]. For numerical stability analysis, the Lyapunov function and the condition for $\mathbf{P}$ has been formulated as a pair of linear matrix inequalities (LMI) for every closed loop system matrix $\mathbf{A}_{cl,reg,i} = \mathbf{A}_{reg} - \mathbf{b}_{reg}\mathbf{k}_i^T$ of the switched active suspension system

$$\left(\mathbf{A}_{cl,reg,i}^T\mathbf{P} + \mathbf{P}\mathbf{A}_{cl,reg,i}\right) < \mathbf{0} \qquad \text{for} \qquad i \in \{1, \ldots, n\} \tag{14}$$

$$\mathbf{P} = \mathbf{P}^T > \mathbf{0}\,. \tag{15}$$

These equations are solved numerically. Although no feasible solution for all six controllers exists, two feasible solutions $\mathbf{P}_1$ and $\mathbf{P}_2$ have been obtained for two subsets of LQR-controllers $\mathbf{k}_i^T$ with $i \in \{1, \ldots, 5\}$ and $\mathbf{k}_j^T$ with $j \in \{3, \ldots, 6\}$. Switching between controllers within each subset thus results in an asymptotically stable system for arbitrary switching signals $\sigma(\cdot)$ because the Lyapunov function is a common quadratic Lyapunov function (CQLF) of all systems within the subset [12].

Soft switching

Because the active suspension system is improper regarding the control input, a discontinuous control force resulting from a noncontinuous switching function $\sigma(q_{adp}(t),\ q_{susp}(t))$ would result in discontinuities of $\ddot{z}_c$ and thus decreasing passenger comfort. To avoid these discontinuities "soft" switching by interpolating between the controllers via $q_{adp}(t)$ and $q_{susp}(t)$ directly is preferable. Therefore, stability for linear interpolation between the state feedback controllers is analyzed.

Theorem 1. *If two closed loop system matrices* $\mathbf{A}_1$ *and* $\mathbf{A}_2$ *resulting from control loops with different state feedback controllers* $\mathbf{K}_1$ *and* $\mathbf{K}_2$ *for the same open loop system matrix* $\mathbf{A}_{ol}$ *have a CQLF characterized by* $\mathbf{P} : \mathbf{P} = \mathbf{P}^T > \mathbf{0}$*, the system matrix*

$$\mathbf{A}_{cl} = \mu\mathbf{A}_1 + (1-\mu)\mathbf{A}_2\ , \quad 0 \le \mu \le 1 \tag{16}$$

being a linear interpolation of $\mathbf{A}_1$ *and* $\mathbf{A}_2$ *has the same CQLF characterized by* $\mathbf{P}$.

Proof. A CQLF of the two closed loop systems is defined by

$$\exists \mathbf{P} : \mathbf{A}_i^T\mathbf{P} + \mathbf{P}\mathbf{A}_i < \mathbf{0}\ , \quad \mathbf{P} = \mathbf{P}^T > \mathbf{0} \quad \forall i \in \{1,2\}\ . \tag{17}$$

If we add the scaled Lyapunov functions for the closed loop system matrices we get

$$\mu \underbrace{(\mathbf{A}_1^T\mathbf{P} + \mathbf{P}\mathbf{A}_1)}_{<\mathbf{0}} + (1-\mu)\underbrace{(\mathbf{A}_2^T\mathbf{P} + \mathbf{P}\mathbf{A}_2)}_{<\mathbf{0}} < \mathbf{0}\ . \tag{18}$$

For state feedback $\mathbf{u} = -\mathbf{K}_i\mathbf{x},\ i \in \{1,2\}$ the closed loop system matrices have the form $\mathbf{A}_i = \mathbf{A}_{ol} - \mathbf{B}\mathbf{K}_i$. Considering this and the fact that linear interpolation between the controllers $\mathbf{K}_i$ would result in the state feedback gain matrix $\tilde{\mathbf{K}} = \mu\mathbf{K}_1 + (1-\mu)\,\mathbf{K}_2$, Eq. (18) can be transformed into

$$[\mathbf{A}_{ol} - \mathbf{B}\tilde{\mathbf{K}}]^T\mathbf{P} + \mathbf{P}[\mathbf{A}_{ol} - \mathbf{B}\tilde{\mathbf{K}}] < \mathbf{0}\ . \tag{19}$$

□

Multiple Lyapunov function approach for stable suspension deflection control

Because no CQLF could be obtained for the whole set of closed loop suspension system matrices $\mathbf{A}_{cl,reg,i}$, the stability for the switching control using all six controllers can be ensured using a multiple Lyapunov function approach, [12]. Asymptotic stability in the sense of Lyapunov while switching smoothly between the two numerically calculated Lyapunov functions $V_1(\mathbf{x})$ and $V_2(\mathbf{x})$ is ensured by two conditions:

1. Switching between the two Lyapunov functions is only allowed if the LQR-controller being activated by the switching is either $\mathbf{k}_3^T$, $\mathbf{k}_4^T$ or $\mathbf{k}_5^T$ because both Lyapunov functions are valid for these controllers.

2. It is only allowed to switch back to the Lyapunov function $V_l(\mathbf{x})$ with $l \in \{1, 2\}$ at time t_2 if the associated Lyapunov function has decreased since leaving it at time t_1 (with $t_1 < t_2$), i.e. $V_l(\mathbf{x}(t_2)) < V_l(\mathbf{x}(t_1))$ [12].

Due to the same quadratic structure of $V_1(\mathbf{x})$ and $V_2(\mathbf{x})$ for our control problem, it is sufficient if condition 2 is fulfilled for $l = 1$ to guarantee asymptotic stability.

Switching to $V_2(\mathbf{x})$ is only necessary if the suspension deflection controller $\mathbf{k}_6^T$ should be activated. Ensuring that condition 1 is satisfied, the wheel load adaptation parameter $q_{adp}(t)$ is smoothly increased automatically between $0.66 \leq q_{susp}(t) \leq 0.77$ (see Figure 5) such that $q_{adp}(t)$ is at the lower limit ($q_{adp}(t) = 0.5$) of the activation of controller $\mathbf{k}_3^T$ at least before the suspension controller $\mathbf{k}_6^T$ is enabled to be switched to. For $0.8 \leq q_{susp}(t) \leq 0.9$ the suspension controller $\mathbf{k}_6^T$ is definitely activated (with a similar function as $f(\frac{z_c - z_w}{|\Delta \hat{z}|})$ in Figure 5). Switching back to $V_1(\mathbf{x})$ is only possible if $q_{susp}(t) < 0.77$ and additionally condition 2 is fulfilled for $l = 1$.

5 Simulation Results

The performance of the designed controller is compared to that of a conventional, comfort focussed LQR-controller with $\mathbf{Q}_{y,LQR} = diag\left(2.5 \cdot 10^4,\ 0,\ 0.4,\ 0\right)$ and the passive suspension. As excitation signal $z_g(t)$ a superposition of two synthetic signals (bumps) and two subsequent real measured road track signals is used (Figure 6). The road excitation is zero for all points in time not depicted. Figure 7 shows that the power spectral density (PSD) of $\ddot{z}_c$ is significantly reduced in the range of the chassis' resonance frequency (approx. 1.41 Hz). In the frequency range from 4–8 Hz the adaptive controller performs best concerning comfort (approx. 17% better than the passive suspension and 8% better than the LQR-controller). The comfort gain vs. the LQR-controller would be more significant if a fully active suspension model without passive suspension would be considered. Only the adaptive controller keeps the suspension deflection limit at the first bump.

The proposed road adaptive controller achieves a comfort gain in an rms-sense of approx. 20% in comparison to the passive system and of 11% compared to the LQR-controller for the simulated road profile (Table 3). All control forces are in an acceptable range.

Table 3 Performance of the road adaptive controller.

Quantity	Unit	Passive	LQR	Road adaptive	Comment
$\|\ddot{z}_c\|_{rms}$	$\frac{\mathrm{m}}{\mathrm{s}^2}$	3.06	2.75	2.45	
$\|g_c * \ddot{z}_c\|_{rms}$	$\frac{\mathrm{m}}{\mathrm{s}^2}$	2.85	2.56	2.36	
$\|F_{dyn}\|_{rms}$	N	960.29	855.26	871.36	Limit: $\Gamma_{var} = 938.49$ N
$\|F(t)\|_{rms}$	N	-	156.19	262.66	
$\max(\|F(t)\|)$	N	-	2781	1771	

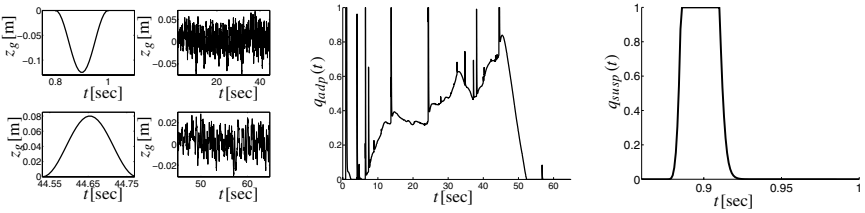

Fig. 6 Road signal $z_g(t)$ (left) and adaptation parameters $q_{adp}(t)$ (middle), $q_{susp}(t)$ (right).

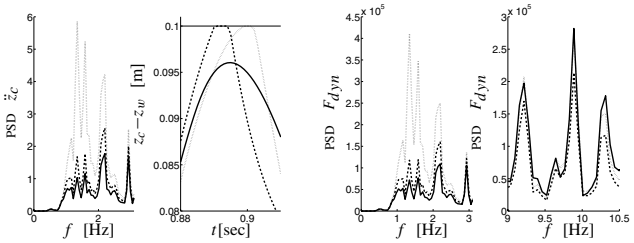

Fig. 7 Power spectral density (PSD) of the chassis acceleration $\ddot{z}_c$ (left), suspension deflection $z_c - z_w$ at the first bump (middle left), power spectral density of the wheel load $\ddot{z}_c$ for two frequency ranges (right); Adaptive controller (solid), LQR-controller (small dots), passive setting (large dots).

6 Conclusion

A road adaptive suspension controller has been designed that switches smoothly between different LQR-controllers depending on the current dynamic wheel load and suspension deflection. The primary control objective is to maximize passenger comfort while given limits for the dynamic wheel load and suspension deflection are not violated. Stability of the system is guaranteed by a multiple Lyapunov function approach implemented in the scheduling algorithm. The result is a performance gain of approx. 20% vs. the passive system and 11% vs. the LQR-controlled suspension. Only the road adaptive controller does not exceed the suspension limit.

References

1. I. J Fialho and G. J. Balas. Road adaptive active suspension design using linear parameter-varying gain-scheduling. *IEEE Transact. on Control Systems Technology*, 10(1):43–54, 2002.
2. D. Hrovat. Survey of advanced suspension developments and related optimal control aplications. *Automatica*, 33(10):1781–1817, 1997.
3. International Standard Organization. *ISO 2631-1:1997 – Mechanical Vibration and Shock – Evaluation of Human Exposure to Whole-Body Vibration*, 1997.
4. J. Lin and I. Kanellakopoulos. Nonlinear design of active suspensions. In *Proceedings of the 34th IEEE Conference on Decision and Control, New Orleans, LA*, pp. 3567–3569, 1995.

5. J. Lin and I. Kanellakopoulos. Road-adaptive nonlinear design of active suspensions. In *Proc. American Control Conference*, 1997.
6. G. Ludyk. *Theoretische Regelungstechnik 2*. Springer, Berlin, 1995.
7. M. Mitschke and H. Wallentowitz. *Dynamik der Kraftfahrzeuge*. Springer, Berlin, 2004.
8. J. J. E. Slotine and W. Li. *Applied Nonlinear Control*. Prentice Hall, Englewood Cliffs, NJ, 1991.
9. P. Venhovens. *Optimal Control of Vehicle Suspensions*. Delft University of Technology, Faculty of Mechanical Engineering, Delft, 1993.
10. T. L. Paez, P. H. Wirsching, and K. Ortiz. *Random Vibrations – Theory and Practice*. John Wiley and Sons, New York, 1995.
11. J. Y. Wong. *Theory of Ground Vehicles*. John Wiley & Sons, New York, 2001.
12. K. Wulff. *Quadratic and Non-Quadratic Stability Criteria for Switched Linear Systems*. PhD Thesis, National University of Ireland, Department of Computer Science, Maynooth, 2004.